SCIENTIFIC REPORTS

OPEN

SUBJECT AREAS:
BIOGEOCHEMISTRY
ENVIRONMENTAL SCIENCES

Received
3 April 2014

Accepted
16 July 2014

Published
11 August 2014

Correspondence and requests for materials should be addressed to A.B. (ab2vb@virginia.edu)

Can land use intensification in the Mallee, Australia increase the supply of soluble iron to the Southern Ocean?

Abinash Bhattachan & Paolo D'Odorico

Department of Environmental Sciences, University of Virginia, Box 400123, Charlottesville, Virginia 22904-4123 USA.

The supply of soluble iron through atmospheric dust deposition limits the productivity of the Southern Ocean. In comparison to the Northern Hemisphere, the Southern Hemisphere exhibits low levels of dust activity. However, given their proximity to the Southern Ocean, dust emissions from continental sources in the Southern Hemisphere could have disproportionate impact on ocean productivity. Australia is the largest source of dust in the Southern Hemisphere and aeolian transport of dust has major ecological, economic and health implications. In the Mallee, agriculture is a major driver of dust emissions and dust storms that affect Southeastern Australia. In this study, we assess the dust generating potential of the sediment from the Mallee, analyze the sediment for soluble iron content and determine the likely depositional region of the emitted dust. Our results suggest that the Mallee sediments have comparable dust generating potential to other currently active dust sources in the Southern Hemisphere and the dust-sized fraction is rich in soluble iron. Forward trajectory analyses show that this dust will impact the Tasman Sea and the Australian section of the Southern Ocean. This iron-rich dust could stimulate ocean productivity in future as more areas are reactivated as a result of land-use and droughts.

Satellite observations show that the most active dust sources on Earth are in the Northern Hemisphere[1,2], which accounts for 80 to 90% of the global dust emissions[3], while the Southern Hemisphere exhibits relatively low dust concentrations. Atmospheric dust is an important source of iron to the high nutrient low chlorophyll (HNLC) waters of the Southern Ocean[4,5], although upwelling[6] and hydrothermal activity[7] are also considered to be important contributors. Because of the low rates of atmospheric dust deposition in the Southern Hemisphere, the productivity of the Southern Ocean is constrained by the limited supply of soluble iron[6,8,9]. It has been argued that fluctuations of atmospheric CO_2 concentrations during glacial-interglacial transitions can be explained by changes in supply of iron in dust[10,11] resulting from changes in dust emissions associated with periods of aridification or revegetation in continental land masses[12].

Presently, the main active dust sources in the Southern Hemisphere include the Lake Eyre Basin in Australia, the Makgadikgadi and Etosha pans in southern Africa, and the Salar de Uyuni region in Bolivia[13]. Land-use practices such as deforestation and overgrazing have potential to activate new dust sources in the Southern Hemisphere[14,15] with significant impacts to downwind soils and ecosystems. Potential new dust sources that could be activated as an effect of land use have been identified in Patagonia[14], the Kalahari[16], while in Australia the effect of land use on dust emissions has seldom been investigated in the context of its impact on ocean productivity.

Even though the contribution by dust sources in the Southern Hemisphere to the global dust budget is minimal, these sources could have disproportionately large global impact given the proximity to the Southern Ocean[4]. Therefore Australia is an ideal laboratory to study the connection between wind erosion, dust transport and ocean productivity. One of the largest dust sources in the Southern Hemisphere[13,17], Australia plays an important role in the supply of dust to the Southern Ocean[11,18] and adjacent marine and terrestrial systems[19–22]. Dust storms in Australia generally coincide with periods of drought[23–25], and these events can pose serious threats to local economy and human health[13,26]. For example, it has been estimated that the September 2009 dust storm in New South Wales caused $299 millions in economic damage[27]. The impact of soil erosion is often manifested also in a reduction of soil fertility and agricultural productivity[28]. The increased frequency of dust storms has detrimental effects on human health[29]; for example dust combined with bushfire smoke led to increased mortality in Sydney[30] and widespread respiratory illnesses[31].

Table 1 | Study sites in the Mallee. The grain size distribution was analyzed for a subsample of the soil collected from the study sites

Site	Latitude (°S)	Longitude (°E)	% clay	% silt	% sand
Dune Crest 1	35.004619	143.248805	1	8	91
Dune Crest 3	35.005234	143.265465	2	8	90
Dune Crest 5	34.993001	143.258671	2	6	92
Interdune 2	35.005002	143.249927	3	14	83
Interdune 4	35.006978	143.270734	4	20	76
Interdune 6	34.994540	143.263006	2	11	87
Salt Pan	35.226154	143.433129	1	15	84
Little Desert National Park	36.527164	142.015167	1	3	96

It is believed that Australia was a significant source of dust during the Last Glacial Maximum[32], when increased aridity caused intense deflation of sediments from the continental sources to the Tasman Sea[33]. Satellite records suggest that the Lake Eyre Basin is the primary dust source in Australia[1,2] and episodic dust activity is seen in the Strzelecki Desert[1,34]. Central Australia and the Mallee within the Murray-Darling Basin are identified as other dust sources[35]. Although evidence of the extent of wind erosion in the Mallee can be found in land degradation surveys as early as the 1930s[36], very little is known about the amount of dust that can be emitted from the Mallee. Numerous studies have investigated the impacts of Australian dust on Southern Ocean biogeochemistry[5,37–39] or adjacent marine systems[22,39] however, it is unclear how dust emissions from the Mallee might affect the supply of iron and likely affect the productivity of the Southern Ocean. To this end, this study will assess the dust generating potential of the sediments from the Mallee, analyze the soluble iron content in the dust-sized fraction of the sediments and determine the likely deposition region of the emitted dust. Other studies[15,40] have shown that the use of a laboratory dust generator could allow for assessing the potential of sediments to emit dust.

Results

The grain size analysis shows that sediments from the Mallee are sandy with interdunes rich in silt-sized fractions (Table 1). To place these numbers in the broader context of dust emissions potentially supplying iron to the Southern Ocean, we ran the dust generator for sediments from dust sources in Southern Africa, including the southern Kalahari interdunes that could be activated by overgrazing and climate change[15], as well as the currently active dust sources of the Makgadikgadi and Etosha pans (Figure 1a). The dust generating potential for sediments from interdunes and dune crests from the agricultural fields of the Mallee region is greater than the salt pan and the Little Desert (Table 2, Figure 1b). PM_{10} concentrations were on average 74.86 mg m^{-3} for the dune crests and 80.4 mg m^{-3} for interdunes. The PM_{10} concentration of the Little Desert soil is at

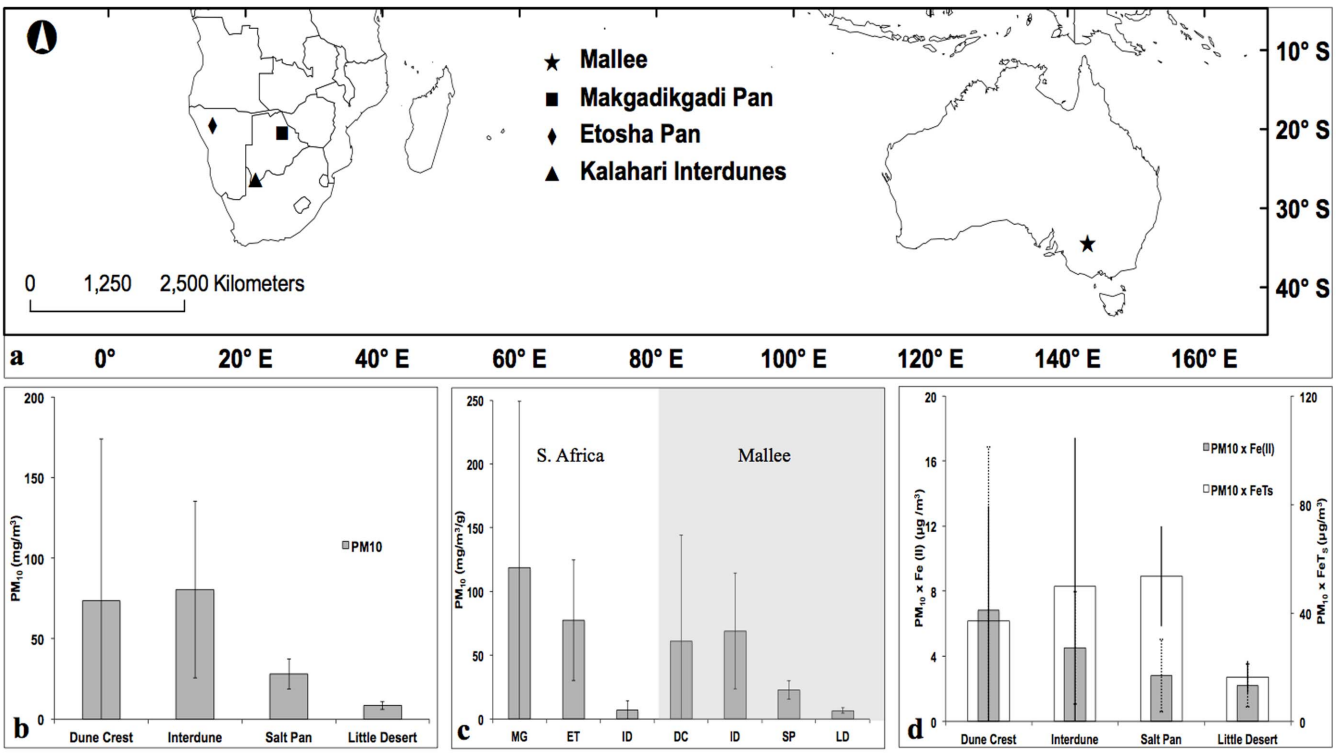

Figure 1 | (a) Map of the Southern Hemisphere dust sources included in this study (b) PM_{10} concentration (mg m^{-3}) from the dust generation experiments with ±1 standard deviation. PM_{10} values from Little Desert Transect are aggregated. (c) The dust potential per unit mass (mg m^{-3} g^{-1}, with ±1 standard deviation) for the Makgadikgadi Pan (MG), Etosha Pan (ET), southern Kalahari interdunes (ID) and the Mallee dune crests (DC), interdune (ID), salt pan (SP) and little desert (LD) (d) Iron-in-dust potential (μg m^{-3}, with ±1 standard deviation) is calculated by multiplying PM10 concentration with the ferrous ion, Fe(II) (grey bars) and with total soluble iron (FeTS) (white bars). (Information on the PM_{10} concentration from Southern African dust sources are available in Supplementary Table S1). This map was created in ArcGIS (ESRI, Redlands, CA).

Table 2 | PM_{10} values from the dust generator experiment (with ±1 standard deviation)

Site	PM_{10} (mg m^{-3})
Dune Crest 1	139.67 ± 172.63
Dune Crest 3	48.65 ± 5.65
Dune Crest 5	33.26 ± 19.08
Interdune 2	69.58 ± 5.39
Interdune 4	128.45 ± 78.07
Interdune 6	43.17 ± 10.94
Salt Pan	28.05 ± 9.26
Little Desert National Park	8.56 ± 0.55

least one order of magnitude smaller than the interdune and dune sediments (Figure 1b).

The southern Kalahari interdunes have the greatest dust generating potential and thus preferred for this comparison than vegetated dune crests and bare dunes in the region[15]. A comparison of dust concentration per unit mass (only for PM_{10}) between the Mallee and the Southern African sediments reveals that the Makgadikgadi Pan sediments have the highest potential (~118 mg m^{-3} g^{-1}), followed by the Etosha Pan (~77 mg m^{-3} g^{-1}) and the Mallee soils (~61 mg m^{-3} g^{-1} for the dune crests and 69 mg m^{-3} g^{-1} for interdunes) (Figure 1c). The southern Kalahari interdunes have a potential of about 7 mg m^{-3} g^{-1}. PM_{10} concentration values for sediments collected from the Makgadikgadi Pan (19–435 mg m^{-3} g^{-1}) and the Mallee dune crests (19–281 mg m^{-3} g^{-1}) have a broad range of variability (Figure 1c).

The soluble iron content is higher in the parent soil for both ferrous ion, Fe(II) and total soluble iron, FeT_S (Table 3). The iron contents of soils from dune crests and interdunes are similar in magnitude for both dust fraction and parent soil. The iron-in-dust potential is a useful measure to assess the potential for soluble iron emissions of different dust sources. It can be expressed as the product of the PM_{10} concentration to the iron content in the dust fraction. For Fe(II), the iron-in-dust potential is the greatest in soil from the dune crest, followed by interdunes, salt pan and the little desert sediments (Figure 1d). However, for FeT_S, the salt pan and the interdune sediments have comparable iron-in-dust potential (Figure 1d).

The spatial distribution of the terminal location of the 7-day forward trajectories originating at 500 m a.s.l from the Mallee for the period 1999–2009 shows that the recurrent dust transport pathways from the Mallee are to the South Pacific Ocean (Figure 2).

Discussion

Wind erosion is a major cause of loss of soil resources and land degradation in drylands[26] and its intensification often results from the expansion of agriculture[41]. In Australia, the European colonization led to rapid changes in land use, which contributed to soil erosion and dust emissions[42]. In the case of the Mallee, the driver of degradation was the development of agriculture and overgrazing, which resulted in some of the highest wind erosion rates in Australia[36]. Our results show that the potential of the Mallee soils to emit dust is comparable to other currently active dust sources in the Southern Hemisphere (Figure 1c); the deposition of this iron rich dust could possibly alter the productivity and biogeochemical cycling of the South Pacific Ocean.

The percentage of clay and silt sized particles is greater in the Mallee sediments than in the southern Kalahari interdunes (for southern Kalahari grain size data see Bhattachan et al.[16]). However, we note that the percentage of clay and silt sized particles in soil is not a robust measure of dust generating potential of a source and other mechanisms such as sandblasting, and breaking up of loose aggregates during erosion could affect the dust generating potential[43]. Thus, while a laboratory dust generator is useful in quantifying the amount of dust that can be generated by soil from different sources, it cannot simulate the effect of saltation on dust generation. The dust generating potential of the Mallee soil (both dune crests and interdunes) is much greater than the southern Kalahari interdunes (Figure 1c). The Little Desert Transect has the smallest dust potential compared to the interdune and dune sediments however, the dust generating potential of the well-managed farmlands in southern Kalahari is equal to soil found in the protected and managed Little Desert National Park (Figure 1c). It is also interesting to note that the salt pan in the Mallee does not have a high dust generating potential, unlike the salt pans of Southern Africa. This low dust generating potential of the salt pan sediments in the Mallee could be attributed to the lack of ephemeral streams and lunette dunes that supply sediments rich with fine particles, which are prevalent in the Makgadikgadi and Etosha Pans.

The Fe(II) content in the dust fraction between the sediments from the Mallee interdunes and the southern Kalahari interdunes are equal whereas FeT_S is slightly greater in soil in the Mallee[44]. Because soils in Australia are highly weathered, any iron present in such soils is likely to be in hematite and goethite forms, with low amount of ferrihydrite, which in fact is the most labile form of iron oxide[23]. Mackie et al.[45] suggest that ground-based processes such as weathering, and abrasion are credited for low amount of ferrihydrite in dust from Australian sources and any ferrihydrite that is left, it is either transformed to hematite or goethite[23] or lost during saltation because of aeolian abrasion[46,47]. It is suggested that soluble form of iron is likely to be redistributed to smaller grains during saltation[45]. Our results show that iron present in the Mallee soil is bound in the coarse fraction (Table 3) and the potential of sand grains emitting iron rich fine particles during entrainment could be high. Furthermore, when dust is transported, atmospheric processing especially in clouds is likely to enhance the solubililty and therefore bioavailability of iron[48,49].

The dust-storm frequency in Australia reaches the highest during austral spring and summer[50] and the main pathway for dust leaving Australia is over the Tasman Sea and south over the Southern Ocean[21,38,39]. It has been suggested that the deposition of iron-rich Australian dust in the HNLC waters of the Southern Ocean could impact its productivity[5]. However, in some cases, phytoplankton

Table 3 | Soluble ferrous, Fe(II) and total soluble iron, FeTs content in mg g^{-1} of Mallee sediments (with ±1 standard deviation). D denotes the fine fraction less than 45 μm and P is the parent soil

Site	$Fe(II)_D$ (mg g^{-1})	$FeTs_D$ (mg g^{-1})	$Fe(II)_P$ (mg g^{-1})	$FeTs_P$ (mg g^{-1})
Dune Crest 1	0.08 ± 0.03	0.17 ± 0.17	0.39 ± 0.23	1.38 ± 0.10
Dune Crest 3	0.10 ± 0.05	0.43 ± 0.64	1.41 ± 0.39	1.87 ± 0.01
Dune Crest 5	0.09 ± 0.06	1.63 ± 0.65	0.55 ± 0.72	1.69 ± 0.22
Interdune 2	0.05 ± 0.01	0.14 ± 0.10	0.17 ± 0.11	1.66 ± 0.17
Interdune 4	0.07 ± 0.05	1.01 ± 0.97	0.08 ± 0.02	1.88 ± 0.04
Interdune 6	0.05 ± 0.06	1.18 ± 0.72	0.44 ± 0.21	1.67 ± 0.08
Salt Pan	0.09 ± 0.04	1.90 ± 0.03	0.11 ± 0.07	1.88 ± 0.02
Little Desert National Park	0.24 ± 0.10	1.88 ± 0.19	1.97 ± 0.39	2.09 ± 0.29

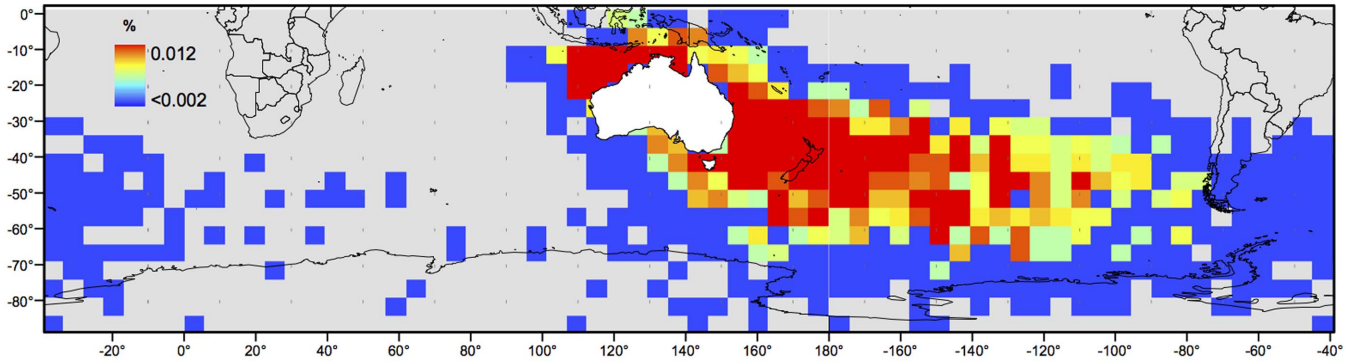

Figure 2 | The spatial distribution of 7-day forward trajectories between 1999–2009 origininating from the Mallee initiated at 500 m a.s.l. The percentages are calculated with the total number of terminations in a 5° by 5° grid. This map was created in ArcGIS (ESRI, Redlands, CA).

response was undetected after major dust storms[18,23] likely because the timing of the event and light availability, which are other important factors controlling ocean productivity. In fact, the deposition of dust is expected to stimulate blooms later in spring or summer when the ocean is more receptive and light is available[39,51]. Our results from the forward trajectory analysis (Figure 2) show that dust from the Mallee has higher probability of depositing over the Tasman Sea and the Subantartic Water Ring Province, which is consistent with other studies[17,21,38,39]. Dust from other sources in Australia, for example, the Lake Eyre Basin (the largest dust source within Australia), however, predominately travels towards the northwest shelf and Great Barrier Reef and not to the Southern Ocean (south of 45° S)[51]. Hence, an increase in dust emissions from the Mallee of the Murray-Darling Basin could have significant impacts on the productivity of the Tasman Sea, and the Southern Ocean.

There is some evidence that dunes in Australia can emit dust, particularly after fire induced vegetation loss[52,53]. Within the Lake Eyre Basin, only 4% of the emissions originated from the actual lakebed whereas dunes accounted for 37% of the plumes[52]. Loss of vegetation cover resulting from increased aridification[54] and land use (e.g., agriculture, overgrazing) has also been related to the remobilization of stabilized dunefields and enhanced dust emissions in the southern Kalahari[16]. Given the potentially strong coupling between Australian land-use practices, dust emissions, and iron delivery to the HNLC waters of the Southern Hemisphere, intensification of agriculture and land degradation in Australia (and the Mallee in particular) could result in an increase in ocean productivity in the South Pacific Ocean.

Methods

Study sites. Triplicated soil samples (about 50 g) were collected from the top 2 cm of soil from six agricultural sites and a salt pan in the Mallee region (Supplementary Figure S1a). These sites are about 2 km away from the banks of the Murray River in an area with a gently rolling topography resulting from relict dunes (Table 1). Additional sampling was performed in the Little Desert National Park (Victoria, Australia) in a duneland that is currently stabilized by grass and woody vegetation (Supplementary Figure S1b). The study site locations for soil samples collected from the southern Kalahari interdunes, and the Makgadikgadi and Etosha Pans are included in supplementary table S1. The grain size distribution of the Mallee soils was measured on a subsample run through a laboratory particle size analyzer (LS 13 320, Beckman Coulter®).

Dust generator. The dust generating potential of the samples collected in the Mallee region of southern Australia and the existing and potential dust sources in Southern Africa was determined using a laboratory dust generator (Custom Products, Big Spring, TX) (Supplementary Figure S1c). Each run was performed with approximately 1 g of soil sample placed in a tube, which rotates around a horizontal pivot axis at the speed of 13 rounds per minute with a 4 s pause between each rotation. A pump draws air from the rotating tube at a rate of 14 L per minute. When the tube is in motion, the sediment falls to the bottom of the tube thereby generating dust. The entrained dust is drawn into the settling chamber where dust concentrations are measured by a dust sensor attached to an aerosol spectrometer (Grimm, Model 1.108). The data units used by the spectrometer are in particle count per liter for particle diameters ranging between 0.3 and 20 μm. The conversion from particle count per liter to concentration (mg m^{-3}) is performed as described in Bhattachan et al.[15]. PM_{10} values (particulate matter less than 10 μm in diameter; expressed in mg m^{-3}) are reported in table 2 and table S1.

Soluble iron. The samples were sieved through a 45 μm sieve to separate the dust sized fraction from the parent soil. The dust fraction and parent soil were then analyzed for total soluble iron, FeT_s and soluble ferrous ion, Fe(II). To determine the soluble iron content, 10 ml of 0.5 M HCl were added to 0.25 g of sample and the solution was shaken for an hour, filtered through a nucleopore filter to eliminate particulate matter. An acetate buffer was used to raise the pH to 5.5 and a 0.1 M ferrozine was added to the solution to measure the Fe(II) content on a UV photospectrometer (Shimadzu 4100) at 562 nm[55]. FeTs was measured using the above method after reduction of Fe(II) by adding 0.01 M of hydroxylamine hydrochrolide.

Forward trajectory analysis. The 7-day forward trajectories were determined using Hybrid Singe Particle Langrangian Integrated Trajectory Model (HYSPLIT)[56], originating from a point within the Mallee (35.013256° S, 143.255357° E) for years 1999 to 2009. The model used NCEP/NCAR reanalysis dataset for years 1999–2005 and the GDAS1 data for years 2006–2009. Forward trajectories were run at altitude of 500 a.s.l. every day at 05 UTC.

1. Prospero, J. M., Ginoux, P., Torres, O., Nicholson, S. E. & Gill, T. E. Environmental characterization of global sources of atmospheric soil dust identified with the Nimbus 7 Total Ozone Mapping Spectrometer (TOMS) absorbing aerosol product. *Rev. Geophys.* **40**, 31, doi:10.1029/2000rg000095 (2002).
2. Washington, R., Todd, M., Middleton, N. J. & Goudie, A. S. Dust-storm source areas determined by the total ozone monitoring spectrometer and surface observations. *Ann. Assoc. Am. Geog.* **93**, 297–313, doi:10.1111/1467-8306.9302003 (2003).
3. Ginoux, P. *et al.* Sources and distributions of dust aerosols simulated with the GOCART model. *J. Geophys. Res.* **106**, 20255 (2001).
4. Jickells, T. D. *et al.* Global iron connections between desert dust, ocean biogeochemistry, and climate. *Science* **308**, 67–71, doi:10.1126/science.1105959 (2005).
5. Cassar, N. *et al.* The Southern Ocean biological response to Aeolian iron deposition. *Science* **317**, 1067–1070, doi:10.1126/science.1144602 (2007).
6. Debaar, H. J. W. *et al.* Importance of iron for plankton blooms and carbon-dioxide drawdown in the Southern Ocean. *Nature* **373**, 412–415, doi:10.1038/373412a0 (1995).
7. Tagliabue, A. *et al.* Hydrothermal contribution to the oceanic dissolved iron inventory. *Nature Geosci.* **3**, 252–256, doi:10.1038/ngeo818 (2010).
8. Martin, J. H. & Fitzwater, S. E. Iron-deficiency limits phytoplankton growth in the Northeast Pacific Subantartic. *Nature* **331**, 341–343, doi:10.1038/331341a0 (1988).
9. Martin, J. H. *et al.* Testing the Iron Hypothesis in ecosystems of the Equatorial Pacific Ocean. *Nature* **371**, 123–129, doi:10.1038/371123a0 (1994).
10. Martin, J. H. Glacial-Interglacial CO2 Change: The Iron Hypothesis. *Paleoceanogr.* **5**, 1–13, doi:10.1029/PA005i001p00001 (1990).
11. Mahowald, N. *et al.* Dust sources and deposition during the last glacial maximum and current climate: A comparison of model results with paleodata from ice cores and marine sediments. *J. Geophys. Res.-Atmos.* **104**, 15895–15916, doi:10.1029/1999jd900084 (1999).
12. Ridgwell, A. J. Dust in the Earth system: the biogeochemical linking of land, air and sea. *Phil. Trans. Royal Soc. London A* **360**, 2905–2924, doi:10.1098/rsta.2002.1096 (2002).
13. Goudie, A. & Middleton, N. *Desert dust in the global system.* (Springer Verlag, 2006).

14. McConnell, J. R., Aristarain, A. J., Banta, J. R., Edwards, P. R. & Simoes, J. C. 20th-century doubling in dust archived in an Antartic Peninsula ice core parallels climate change and desertification in South America. *Proc. Nat. Acad. Sci. USA* **104**, 5743–5748 (2007).
15. Bhattachan, A. *et al.* The Southern Kalahari: a potential new dust source in the Southern Hemisphere? *Environ. Res. Lett.* **7**, 7, doi:10.1088/1748-9326/7/2/024001 (2012).
16. Bhattachan, A., D'Odorico, P., Okin, G. S. & Dintwe, K. Potential dust emissions from the southern Kalahari's dunelands. *J. Geophys. Res.- Earth Surf.* **118**, 307–314 (2013).
17. Tanaka, T. Y. & Chiba, M. A numerical study of the contributions of dust source regions to the global dust budget. *Global Planet. Change* **52**, 88–104, doi:10.1016/j.gloplacha.2006.02.002 (2006).
18. Boyd, P. W. *et al.* Episodic enhancement of phytoplankton stocks in New Zealand subantarctic waters: Contribution of atmospheric and oceanic iron supply. *Global Biogeochem. Cy.* **18**, 23, doi:10.1029/2002gb002020 (2004).
19. Knight, A. W., McTainsh, G. H. & Simpson, R. W. Sediment loads in an Australian dust storm - implications for present and past dust processes. *Catena* **24**, 195–213, doi:10.1016/0341-8162(95)00026-o (1995).
20. Marx, S. K., Kamber, B. S. & McGowan, H. A. Provenance of long-travelled dust determined with ultra-trace-element composition: a pilot study with samples from New Zealand glaciers. *Earth Surf. Proc. Land.* **30**, 699–716, doi:10.1002/esp.1169 (2005).
21. McGowan, H. A., Kamber, B., McTainsh, G. H. & Marx, S. K. High resolution provenancing of long travelled dust deposited on the Southern Alps, New Zealand. *Geomorph.* **69**, 208–221, doi:10.1016/j.geomorph.2005.01.005 (2005).
22. Shaw, E. C., Gabric, A. J. & McTainsh, G. H. Impacts of aeolian dust deposition on phytoplankton dynamics in Queensland coastal waters. *Mar. Freshwater Res.* **59**, 951–962, doi:10.1071/mf08087 (2008).
23. Mackie, D. S. *et al.* Biogeochemistry of iron in Australian dust: From eolian uplift to marine uptake. *Geochem. Geophys. Geosys.* **9**, 24, doi:10.1029/2007gc001813 (2008).
24. McTainsh, G., Chan, Y. C., McGowan, H., Leys, J. & Tews, K. The 23rd October 2002 dust storm in eastern Australia: characteristics and meteorological conditions. *Atmos. Environ.* **39**, 1227–1236, doi:10.1016/j.atmosenv.2004.10.016 (2005).
25. Shao, Y. & Leslie, L. M. Wind erosion prediction over the Australian continent. *J. Geophys. Res.- Atmos.* **102**, 30091–30105 (1997).
26. Ravi, S. *et al.* Aeolian processes and the biosphere. *Rev. Geophys.* **49**, doi:Rg3001 10.1029/2010rg000328 (2011).
27. Tozer, P. & Leys, J. Dust storms - what do they really cost? *Rangeland J.* **35**, 131–142, doi:10.1071/rj12085 (2013).
28. Pimentel, D. *et al.* Environmental and economic costs of soil erosion and conservation benefits. *Science* **267**, 1117–1122 (1995).
29. Goudie, A. S. Desert dust and human health disorders. *Environ. Internat.* **63**, 101–113 (2014).
30. Johnston, F., Hanigan, I., Henderson, S., Morgan, G. & Bowman, D. Extreme air pollution events from bushfires and dust storms and their association with mortality in Sydney, Australia 1994–2007. *Environ. Res.* **111**, 811–816, doi:10.1016/j.envres.2011.05.007 (2011).
31. Merrifield, A., Schindeler, S., Jalaludin, B. & Smith, W. Health effects of the September 2009 dust storm in Sydney, Australia: did emergency department visits and hospital admissions increase? *Environ. Health* **12**, 7, doi:10.1186/1476-069x-12-32 (2013).
32. Bullard, J. E. & McTainsh, G. H. Aeolian-fluvial interactions in dryland environments: examples, concepts and Australia case study. *Prog. Phys. Geog.* **27**, 471–501 (2003).
33. Hesse, P. P. & McTainsh, G. H. Last glacial maximum to early Holocene wind strength in the mid-latitudes of the Southern Hemisphere from aeolian dust in the Tasman Sea. *Quat. Res.* **52**, 343–349 (1999).
34. Mitchell, R. M., Campbell, S. K. & Qin, Y. Recent increase in aerosol loading over the Australian arid zone. *Atmos. Chem. Phys.* **10**, 1689–1699 (2010).
35. McTainsh, G. H. & Pitblado, J. R. Dust storms and related phenomena measured from meteorological records in Australia. *Earth Surf. Proc. Land.* **12**, 415–424, doi:10.1002/esp.3290120407 (1987).
36. McTainsh, G. H., Lynch, A. W. & Burgess, R. C. Wind Erosion in Eastern Australia. *Austral. J. Soil Res.* **28**, 323–339, doi:10.1071/sr9900323 (1990).
37. Bowie, A. R. *et al.* Biogeochemical iron budgets of the Southern Ocean south of Australia: Decoupling of iron and nutrient cycles in the subantarctic zone by the summertime supply. *Global Biogeochem. Cy.* **23**, 14, doi:10.1029/2009gb003500 (2009).
38. Gabric, A. J., Cropp, R., Ayers, G. P., McTainsh, G. & Braddock, R. Coupling between cycles of phytoplankton biomass and aerosol optical depth as derived from SeaWiFS time series in the Subantarctic Southern Ocean. *Geophys. Res. Lett.* **29**, 4, doi:10.1029/2001gl013545 (2002).
39. Gabric, A. J. *et al.* Australian dust storms in 2002–2003 and their impact on Southern Ocean biogeochemistry. *Global Biogeochem. Cy.* **24**, 17, doi:10.1029/2009gb003541 (2010).
40. Singer, A., Zobeck, T., Poberezsky, L. & Argaman, E. The PM10 and PM2.5 dust generation potential of soils/sediments in the Southern Aral Sea Basin, Uzbekistan. *J. Arid Environ.* **54**, 705–728, doi:10.1006/jare.2002.1084 (2003).
41. Lal, R. & Stewart, B. A. *Soil degradation*. Vol. 11 (Springer Verlag, 1990).
42. McTainsh, G. H. & Leys, J. F. in *Land Degradation Processes in Australia* (eds McTainsh, G. H. & Boughton, W. C.) Ch. 7, 188–233 (Longman-Chesire, 1993).
43. Gill, T. E., Zobeck, T. M. & Stout, J. E. Technologies for laboratory generation of dust from geological materials. *J. Hazard. Mat.* **132**, 1–13 (2006).
44. Bhattachan, A., D'Odorico, P. & Okin, G. S. *Biogeochemistry of Southern African Dust.* (in review).
45. Mackie, D., Peat, J., McTainsh, G. H., Boyd, P. & Hunter, K. Soil abrasion and eolian dust production: Implications for iron partitioning and solubility. *Geochem. Geophys. Geosys.* **7** (2006).
46. Bullard, J. E. M. G. H. & Pudmenzky, C. Factors affecting the nature and rate of dust production from natural dune sands. *Sedimento.* **54**, 169–182 (2007).
47. Bullard, J. E. & White, K. Dust production and the release of iron oxides resulting from the aeolian abrasion of natural dune sands. *Earth Surf. Proc. Land.* **30**, 95–106 (2005).
48. Baker, A. & Croot, P. Atmospheric and marine controls on aerosol iron solubility in seawater. *Mar. Chem.* **120**, 4–13 (2010).
49. Mahowald, N. M. *et al.* Atmospheric global dust cycle and iron inputs to the ocean. *Global Biogeochem. Cy.* **19** (2005).
50. McTainsh, G., Lynch, A. & Tews, E. Climatic controls upon dust storm occurrence in eastern Australia. *J. Arid Environ.* **39**, 457–466 (1998).
51. Cropp, R. A. *et al.* The likelihood of observing dust-stimulated phytoplankton growth in waters proximal to the Australian continent. *J. Mar. Sys.* **117**, 43–52 (2013).
52. Bullard, J., Baddock, M., McTainsh, G. & Leys, J. Sub-basin scale dust source geomorphology detected using MODIS. *Geophys. Res. Lett.* **35**, 6, doi:10.1029/200nl033928 (2008).
53. Strong, C. L., Bullard, J. E., Dubois, C., McTainsh, G. H. & Baddock, M. C. Impact of wildfire on interdune ecology and sediments: An example from the Simpson Desert, Australia. *J. Arid Environ.* **74**, 1577–1581, doi:10.1016/j.jaridenv.2010.05.032 (2010).
54. Thomas, D. S. G., Knight, M. & Wiggs, G. F. S. Remobilization of Southern African desert dune systems by twenty-first century global warming. *Nature* **435**, 1218–1221 (2005).
55. Stookey, L. L. Ferrozine-A New Spectrophotometric Reagent for Iron. *Analyt. Chem.* **42**, 779 (1970).
56. Draxler, R. R. & Rolph, G. D. (NOAA Air Resour. Lab, Silver Spring, Md., 2003).

Acknowledgments

This work was funded by the National Science Foundation, through grant EAR 1147545. We are thankful to Noaa Spiekermann and Shamika Ranasinghe for their help with HYSPLIT analysis and Ted Zobeck (USDA-ARS, Lubbock, TX) for sharing with us the design of Lubbock dust generator. We gratefully acknowledge the NOAA Air Resources Laboratory (ARL) for the provision of the HYSPLIT transport and dispersion model and/or READY website (www.arl.noaa.gov/ready.php) used in this publication. This article was published in part thanks to funds provided by the University of Virginia Library Open Access Fund.

Author contributions

A.B. and P.D. designed the study; A.B. performed analysis; and both authors contributed to the interpretation of the results and the writing of the paper.

Additional information

Supplementary information accompanies this paper at http://www.nature.com/scientificreports

Competing financial interests: The authors declare no competing financial interests.

How to cite this article: Bhattachan, A. & D'Odorico, P. Can land use intensification in the Mallee, Australia increase the supply of soluble iron to the Southern Ocean? *Sci. Rep.* **4**, 6009; DOI:10.1038/srep06009 (2014).